

# Massive Quasinormal Modes of a Schwarzschild-de Sitter Black Hole with a Global Monopole

Jia-Feng Chang<sup>1,2,4</sup> and You-Gen Shen<sup>1,2,3,5</sup>

*Received February 10, 2006; accepted May 1, 2006*  
*Published Online: June 7, 2006*

---

Using the WKB approximation, we evaluate both the massless and massive scalar and Dirac fields quasinormal modes (QNMs) of a Schwarzschild-de Sitter black hole. The result shows that the field with higher masses and larger cosmological constant  $\Lambda$  will decay more slowly. We also found that the global monopole is similar to a factor to modify the  $\kappa$  of Dirac field or  $l$  of scalar field, where  $\kappa$  is the angular momentum number of Dirac field, and  $l$  is the angular momentum number of scalar field.

---

**KEY WORDS:** black hole physics; gravitational waves; relativity; QNMs.

---

## 1. INTRODUCTION

It is well-known that there are three stages during the evolution of the field perturbation in black hole background: the initial outburst from the source of perturbation, the quasinormal oscillations and asymptotic tails. The frequencies and damping time of the quasinormal oscillations called “quasinormal modes” are determined only by the black hole’s parameters and independent of the initial perturbations. A great deal of efforts have been devoted to the black hole’s QNMs for the possibility of direct identification of black hole existence through gravitational wave detectors in the near future Kokkotas and Schmidt (1999); Nollert (1999). The study of black hole’s QNMs has a long history, most of the studies immersed in an asymptotically flat space-time. The discovery of the *AdS/CFT* correspondence and the expanding universe motivated the investigation of QNMs

<sup>1</sup> Shanghai Astronomical Observatory, Chinese Academy of Sciences, Shanghai 200030, China.

<sup>2</sup> National Astronomical Observatories, Beijing 100012, China.

<sup>3</sup> Institute of Theoretical Physics, Chinese Academy of Sciences, Beijing 100080, China.

<sup>4</sup> Graduate School of Chinese Academy of Sciences, Beijing 100039, China.

<sup>5</sup> To whom correspondence should be addressed at You-Gen Shen, Shanghai Astronomical Observatory, Chinese Academy of Sciences, 80 Nandan Road, Shanghai 200030, China; e-mail: ygshen@center.shao.ac.cn.

in de Sitter Brady *et al.* (1997, 1999) and anti-de Sitter Horowitz and Gubeny (1999); Cardoso and Lemos (2001); Moss and Norman (2002) space-time in past few years.

In the early universe, phase transitions can give rise to various kinds of topological defects such as monopoles. Monopoles form as a result of a gauge-symmetry breaking which are similar to elementary particles. Most of their energy is concentrated in a small region near the monopole core. Resulting from a global symmetry breaking, global monopole Barriola and Vileikin (1989) has Goldstone field with energy density decreasing with the distance as  $r^{-2}$  and the total energy is linearly divergent at large distances. Large energy in the Goldstone field surrounding global monopole suggests that they can produce strong gravitational field and influence QNMs of the black hole. A black hole with a global monopole is the result of an interesting process in which a black hole swallows a global monopole. It possesses a solid deficit angle which makes it quite different from normal black holes.

Science the QNMs are exponentially damped in time, only the mode corresponding to the fundamental frequency (lowest imaginary part) should up in signal, we calculate the low-lying modes of black holes. Most methods in evaluating the QNMs are numerical in nature. Recently, using the third-order WKB approximation, Cho evaluated the Dirac field QNMs of a Schwarzschild black hole Cho (2002). A powerful WKB scheme was devised by Schutz and Will (1985), and was extended to higher orders in Iyer and Will (1987). Comparing with other approaches, this WKB approximation is accurate for the low-lying modes Iyer (1990). QNMs are the intermediate stage and dominated by low-lying modes. As said early, the QNM frequencies will depend on the black hole parameters, it should be possible to infer the black hole parameters solely from the QNM frequencies.

Recently observational evidence suggests that the universe has a positive cosmological constant. It means the universe responsibly change from asymptotical flat to asymptotical de Sitter space-time. The study of QNMs in asymptotically de Sitter spacetimes has garnered much attention Moss and Norman (2002); Mellor and Moss (1990); Cardoso and Lemos (2003); Molina (2003); Maassen A van den (2003); Suneeta (2003); Zhidenko (2004); Jing (2004). We have evaluated Neutrino QNMs of a Kerr-Newman-de Sitter black hole Chang and Shen (2005).

In this paper, we evaluate the QNMs of a Schwarzschild-de Sitter black hole with a global monopole. We consider the metric of a Schwarzschild-de Sitter black hole with a global monopole in Sect. 2. In Sect. 3, we use the third-order WKB approximation to evaluate the QNMs of massless and massive scalar fields. In Sect. 4 we evaluate the QNMs for Dirac field case. Conclusions and discussions are presented in Sect. 4.

**2. A SCHWARZSCHILD BLACK HOLE WITH A GLOBAL MONOPOLE IN de SITTER SPACE-TIME**

The metric of a Schwarzschild black hole with a global monopole can be written as Barriola and Vileinkin (1989):

$$ds^2 = - \left( 1 - 8\pi\eta^2 - \frac{2M'}{r'} \right) dt'^2 + \left( 1 - 8\pi\eta^2 - \frac{2M'}{r'} \right)^{-1} dr'^2 + r'^2(d\theta^2 + \sin^2\theta d\varphi^2), \tag{1}$$

where  $\eta \ll m_p$  is the scale factor of symmetry-breaking,  $m_p = \sqrt{\frac{\hbar c}{G}}$  is the Planck mass. In the de Sitter space-time, Eq. (1) can be written as

$$ds^2 = - \left( 1 - 8\pi\eta^2 - \frac{2M'}{r'} - \frac{\Lambda'}{3}r'^2 \right) dt'^2 + \left( 1 - 8\pi\eta^2 - \frac{2M'}{r'} - \frac{\Lambda'}{3}r'^2 \right)^{-1} dr'^2 + r'^2(d\theta^2 + \sin^2\theta d\varphi^2). \tag{2}$$

Introduce a change of variables as follows Shen and Chen (1998):

$$t = (1 - 8\pi\eta^2)^{\frac{1}{2}}t', \quad r = (1 - 8\pi\eta^2)^{-\frac{1}{2}}r', \tag{3}$$

$$M = (1 - 8\pi\eta^2)^{-\frac{3}{2}}M', \quad \Lambda = (1 - 8\pi\eta^2)\Lambda'.$$

Equation (2) can be written as

$$ds^2 = -f dt^2 + \frac{1}{f} dr^2 + b^2 r^2 (d\theta^2 + \sin^2\theta d\varphi^2), \tag{4}$$

with

$$f = 1 - \frac{2M}{r} - \frac{\Lambda}{3}r^2, \quad b^2 = 1 - 8\pi\eta^2, \tag{5}$$

where  $M$  is the effective black hole mass and  $\Lambda$  is the positive cosmological constant. In the next two sections, we treat  $M$  as a unit of mass and calculate quasinormal modes of a black hole at  $\Lambda = 0.0225$  and  $b = 0.95$ . Apart from the deficit solid angle  $\Delta = 4\pi b = 32\pi G\eta^2$ , this metric is very similar to the Schwarzschild-de Sitter metric Yu (2002) and the introduction of a global monopole charge does not significantly alter the nature of the Schwarzschild-de Sitter field Dadhich *et al.* (1998).

## 2. QUASINORMAL MODES OF SCALAR FIELD

In the curved space-time, the Klein-Gordon equation is given by

$$\frac{1}{\sqrt{-g}} \partial_\mu (\sqrt{-g} g^{\mu\nu} \partial_\nu \Phi) = m^2 \Phi. \tag{6}$$

Using the ansatz

$$\Phi = e^{-i\omega t} \frac{R(r)}{r} Y(\theta, \varphi), \tag{7}$$

we can obtain the radial equation,

$$\left( \frac{d^2}{dr_*^2} + \omega^2 - V(r) \right) R(r) = 0, \tag{8}$$

where

$$V(r) = \frac{l(l+1)}{b^2 r^2} f + m^2 f + \frac{f f'}{r}, \tag{9}$$

the quantum number of angular momentum  $l$  is positive integers,  $r_*$  is the well known ‘‘tortoise’’ coordinate given by

$$dr_* = \frac{dr}{f}, \tag{10}$$

and

$$f' = \frac{df}{dr}. \tag{11}$$

The WKB approximation developed by Schutz and Will (1985); Iyer and Will (1987); Iyer (1990) has been used extensively in various black hole cases. The formula for the quasinormal modes  $\omega$  in the WKB approximation is given by Iyer and Will (1987)

$$\omega^2 = [V_0 + (-2V_0'')^{1/2} \Delta] - i \left( n + \frac{1}{2} \right) (-2V_0'')^{1/2} (1 + \Omega), \tag{12}$$

where

$$\Delta = \frac{1}{(-2V_0'')^{1/2}} \left\{ \frac{1}{8} \left( \frac{V_0^{(4)}}{V_0''} \right) \left( \frac{1}{4} + \alpha^2 \right) - \frac{1}{288} \left( \frac{V_0'''}{V_0''} \right)^2 (7 + 60\alpha^2) \right\} \tag{13}$$

$$\begin{aligned} \Omega = \frac{1}{(-2V_0'')} & \left\{ \frac{5}{6912} \left( \frac{V_0'''}{V_0''} \right)^4 (77 + 188\alpha^2) - \frac{1}{384} \left( \frac{V_0'''^2 V_0^{(4)}}{V_0''^3} \right) (51 + 100\alpha^2) \right. \\ & + \frac{1}{2304} \left( \frac{V_0^{(4)}}{V_0''} \right)^2 (67 + 68\alpha^2) + \frac{1}{288} \left( \frac{V_0'' V_0^{(5)}}{V_0''^2} \right) (19 + 28\alpha^2) \\ & \left. - \frac{1}{288} \left( \frac{V_0^{(6)}}{V_0''} \right) (5 + 4\alpha^2) \right\}. \tag{14} \end{aligned}$$

Here

$$\alpha = n + \frac{1}{2}, \quad n = \begin{cases} 0, 1, 2, \dots, \text{Re}(\omega) > 0, \\ -1, -2, -3 \dots, \text{Re}(\omega) < 0, \end{cases} \tag{15}$$

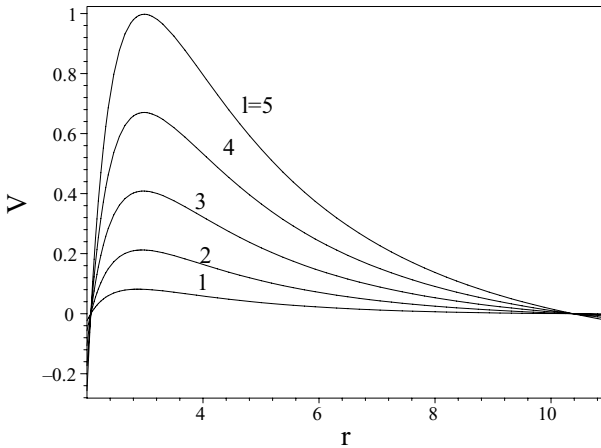
$$V_0^{(n)} = \left. \frac{d^n V}{dr_*^n} \right|_{r_* = r_*(r_{\max})}, \tag{16}$$

$n$  is the mode number and  $n < l$  for low-lying modes.

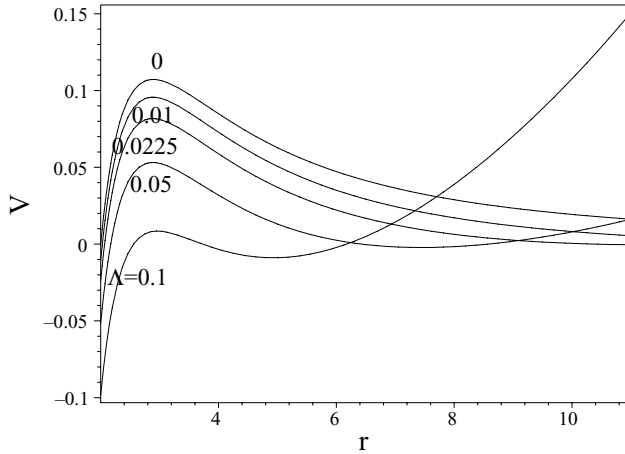
The QNMs are decided by the effective potential. We analyze the dependence of effective potential on parameters  $l, \Lambda, m, b$ . The effective potential  $V$  is in the form of barrier which depends on the values of  $l, \Lambda, m, b$ . The effective potential as a function of  $r$  is plotted for some configurations of  $l, \Lambda, m, b$  in Figs. 1–4. From those figures, we can see that the dependence of  $V$  on  $l, \Lambda, m$  is stronger than on  $b$ , in fact  $b$  changes the value of  $l$  little.

Using WKB approximation to evaluate the QNMs, we plug the effective potential of Eq. (9) into Eq. (12), and obtain the complex QNMs of scalar field. Because there exists cosmological constant  $\Lambda$ , the space-time possesses two horizons: the black hole horizon  $r = r_e$  and the cosmological horizon  $r = r_c$ . While  $r$  varies from  $r_e$  to  $r_c$ , the effective potential  $V$  reduces to zero, so the potential barrier can not turn effectively into a potential step Cho (2002).

In the Fig. 1 we show the dependence of scalar field effective potential of the Schwarzschild-de Sitter black hole with a global monopole on angular momentum number  $l$ . We see the peak value and position of the potential increase with  $l$ .



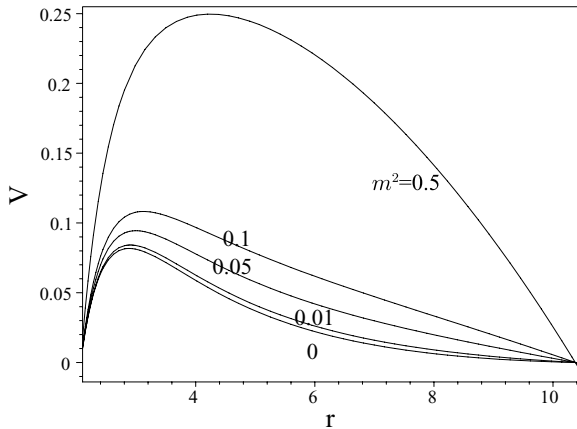
**Fig. 1.** Variation of the effective potential for scalar field with  $\Lambda = 0.0225, b = 0.95, m = 0, l = 1, 2, 3, 4, 5$ .



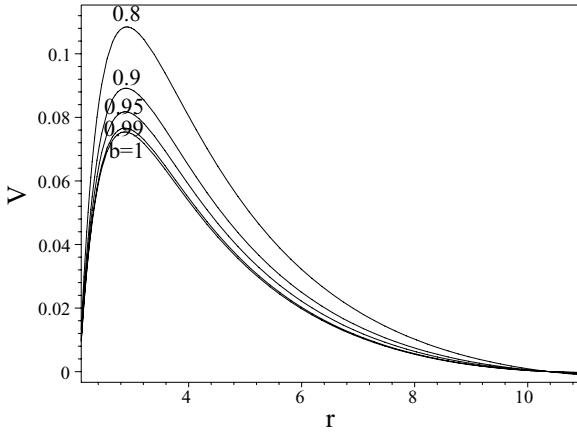
**Fig. 2.** Variation of the effective potential for scalar field with  $b = 0.95, m = 0, l = 1, \Lambda = 0, 0.01, 0.0225, 0.05, 0.1$ .

Figure 2 shows the dependence of effective potential on the cosmological constant  $\Lambda$ . Increasing of  $\Lambda$  reduces the peak value of the effective potential and makes the cosmological horizon  $r_c$  close to the black hole horizon  $r_e$ .

In the Fig. 3, we show the dependence of the effective potential on the mass of scalar field  $m$ . Mass of scalar fields increases the peak value of effective potential. From Fig. 9, we see  $b < 1$  is a factor to modify  $l$ , and the value of  $b$  is close to 1.



**Fig. 3.** Variation of the effective potential for scalar field with  $\Lambda = 0.0225, b = 0.95, l = 1, m = 0, 0.01, 0.05, 0.1, 0.5$ .



**Fig. 4.** Variation of the effective potential for scalar field with  $\Lambda = 0.0225, l = 1, m^2 = 0, b = 1, 0.99, 0.95, 0.9, 0.8$ .

So in the Fig. 4,  $b$  changes the effective potential little and the increasing of  $b$  is similar to the decreasing of  $l$ .

We plot QNMs of scalar fields with different mass for  $\Lambda = 0.0225, b = 0.95$  in Fig. 5. We can see when the mass of the field increases, the real parts of the frequencies increase while the magnitude of imaginary parts decrease. The smaller  $l$  and  $n$ , the more the frequencies will be changed by the mass.

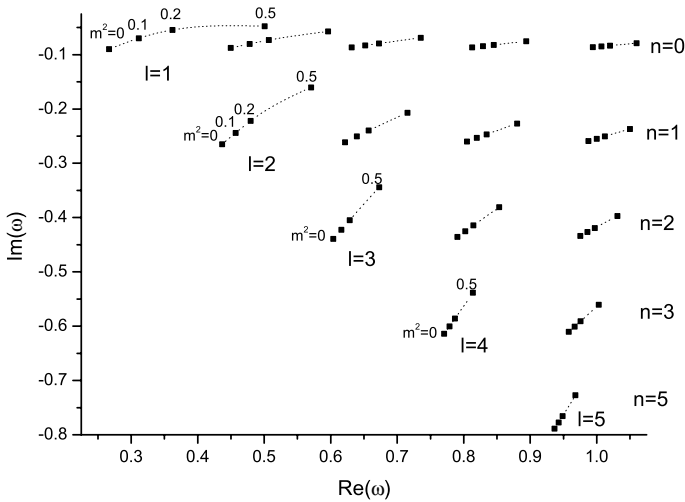


**Fig. 5.** QNMs of scalar field for  $\Lambda = 0.0225, b = 0.95$ .

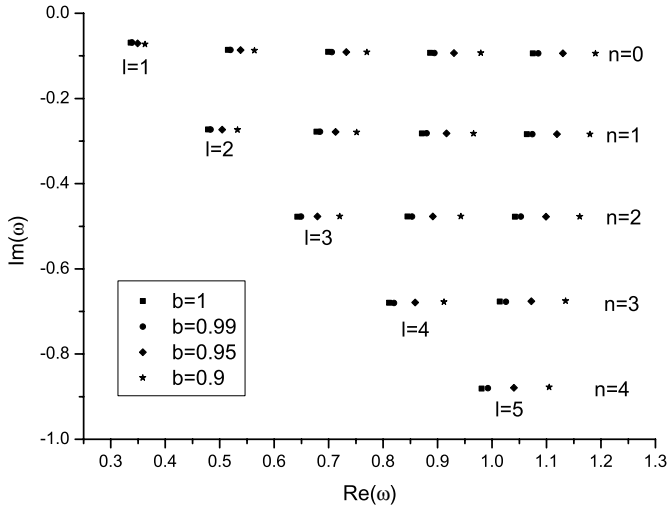


Fig. 6. QNMs of scalar field for  $\Lambda = 0, m^2 = 0.1$ .

We consider the effective potential of  $b$  to the QNMs in Fig. 6. Decreasing of  $b$  means the increasing of  $l$ , which makes the real and the magnitude of imaginary parts of frequencies increase.

In Table I, we compare the frequencies of different value of  $\Lambda$  for  $b = 1$  which means a black hole without a global monopole. The existence of  $\Lambda$  reduces

Table I. QNMs of Scalar Field for  $m^2 = 0.1, b = 1$

$l$	$n$	$\Lambda = 0$	$\Lambda = 0.0009$	$\Lambda = 0.0225$	$\Lambda = 0.09$
1	0	0.336–0.0686i	0.335–0.0683i	0.301–0.0684i	0.139–0.0412i
2	0	0.515–0.0857i	0.5130–0.0855i	0.458–0.0795i	0.218–0.0416i
	1	0.479–0.272i	0.477–0.271i	0.435–0.243i	0.216–0.125i
3	0	0.699–0.0907i	0.696–0.0905i	0.622–0.0826i	0.300–0.0418i
	1	0.677–0.278i	0.675–0.277i	0.608–0.250i	0.298–0.125i
	2	0.642–0.477i	0.640–0.475i	0.583–0.422i	0.296–0.209i
4	0	0.886–0.0929i	0.882–0.0926i	0.789–0.0839i	0.382–0.0418i
	1	0.871–0.282i	0.868–0.280i	0.780–0.253i	0.381–0.126i
	2	0.845–0.477i	0.841–0.475i	0.7612–0.425i	0.379–0.209i
	3	0.811–0.680i	0.808–0.676i	0.736–0.600i	0.376–0.293i
5	0	1.08–0.0940i	1.07–0.0936i	0.959–0.0846i	0.465–0.0419i
	1	1.06–0.284i	1.06–0.282i	0.951–0.254i	0.464–0.126i
	2	1.04–0.477i	1.04–0.475i	0.936–0.426i	0.463–0.210i
	3	1.01–0.677i	1.01–0.674i	0.916–0.601i	0.461–0.293i
	4	0.981–0.881i	0.978–0.877i	0.891–0.777i	0.457–0.377i



both the real parts and the magnitude of imaginary parts of frequencies. Just like mass of the scalar field, the smaller  $l$  and  $n$ , the more the frequencies will be changed by the mass  $\Lambda$ .

### 3. QUASINORMAL MODES OF DIRAC FIELD

According to Brill and Wheeler (1957), the Dirac equation in a general background space-time can be written as

$$[\gamma^a e_a^\mu (\partial_\mu + \Gamma_\mu) + m]\Psi = 0, \tag{17}$$

here  $\gamma^a$  are the Dirac matrices,

$$\gamma^0 = \begin{pmatrix} -i & 0 \\ 0 & i \end{pmatrix}, \quad \gamma^i = \begin{pmatrix} 0 & -i\sigma^i \\ i\sigma^i & 0 \end{pmatrix}, \quad i = 1, 2, 3, \tag{18}$$

while  $\sigma^i$  are the Pauli matrices and  $m$  is the mass of the Dirac field, the four-vectors  $e_a^\mu$  is the inverse of the tetrad  $e_\mu^a$  defined by the metric  $g_{\mu\nu}$ ,

$$g_{\mu\nu} = \eta_{ab} e_\mu^a e_\nu^b, \tag{19}$$

where  $\eta_{ab} = \text{diag}(-1, 1, 1, 1)$  is the Minkowski metric.  $\Gamma_\mu$  are the spin connection coefficients, which are written as

$$\Gamma_\mu = \frac{1}{8}[\gamma^a, \gamma^b] e_a^\nu e_{b\nu;\mu}, \tag{20}$$

here  $e_{b\nu;\mu} = \partial_\mu e_{b\nu} - \Gamma_{\mu\nu}^\alpha e_{b\alpha}$  is the covariant derivative of  $e_{b\nu}$  and  $\Gamma_{\mu\nu}^\alpha$  is the Christoffel symbol.

Taking the tetrad to be

$$e_\mu^a = \text{diag} \left( \sqrt{f}, \frac{1}{\sqrt{f}}, br, br \sin \theta \right), \tag{21}$$

the spin connection coefficients  $\Gamma_\mu$  can be written as

$$\begin{aligned} \Gamma_0 &= \frac{1}{4} \frac{df}{dr} \gamma_0 \gamma_1, & \Gamma_1 &= 0, \\ \Gamma_2 &= \frac{1}{2} \sqrt{f} b \gamma_1 \gamma_2, & \Gamma_3 &= \frac{1}{2} (\sin \theta \sqrt{f} b \gamma_1 \gamma_3 + \cos \theta \gamma_2 \gamma_3). \end{aligned} \tag{22}$$

The Dirac Eq. (17) is changed to be

$$\begin{aligned} -\frac{\gamma_0}{\sqrt{f}} \frac{\partial \Psi}{\partial t} + \sqrt{f} \gamma_1 \left( \frac{\partial}{\partial r} + \frac{1}{r} + \frac{1}{4f} \frac{df}{dr} \right) \Psi + \frac{\gamma_2}{br} \left( \frac{\partial}{\partial \theta} + \frac{1}{2} \cot \theta \right) \Psi \\ + \frac{\gamma_3}{br \sin \theta} \frac{\partial \Psi}{\partial \varphi} + m \Psi = 0. \end{aligned} \tag{23}$$

We simplify Eq. (23) by defining

$$\Psi = f^{-1/4} \Phi, \tag{24}$$

then the Dirac equation becomes

$$\begin{aligned} -\frac{\gamma_0}{\sqrt{f}} \frac{\partial \Phi}{\partial t} + \sqrt{f} \gamma_1 \left( \frac{\partial}{\partial r} + \frac{1}{r} \right) \Phi + \frac{\gamma_2}{br} \left( \frac{\partial}{\partial \theta} + \frac{1}{2} \cot \theta \right) \Phi \\ + \frac{\gamma_3}{br \sin \theta} \frac{\partial \Phi}{\partial \varphi} + m \Phi = 0. \end{aligned} \tag{25}$$

Equation (25) is related to the Dirac equation in flat space-time with central potential Bjorken and Drell (1964). We introduce the tortoise coordinate transformation from the radial variable  $r$  to the tortoise coordinate  $r_*$  and try the ansata,

$$\Phi(t, r, \theta, \phi) = \begin{pmatrix} \frac{iG^{(\pm)}(r)}{r} \phi_{jm}^{\pm}(\theta, \varphi) \\ F^{(\pm)}(r) \phi_{jm}^{\mp}(\theta, \varphi) \end{pmatrix} e^{-i\omega t}, \tag{26}$$

with spinor angular harmonics

$$\phi_{jm}^+ = \begin{pmatrix} \sqrt{\frac{j+m}{2j}} Y_l^{m-1/2} \\ \sqrt{\frac{j-m}{2j}} Y_l^{m+1/2} \end{pmatrix}, \quad \left( \text{for } j = l + \frac{1}{2} \right), \tag{27}$$

$$\phi_{jm}^- = \begin{pmatrix} \sqrt{\frac{j+1-m}{2j+2}} Y_l^{m-1/2} \\ -\sqrt{\frac{j+1+m}{2j+2}} Y_l^{m+1/2} \end{pmatrix}, \quad \left( \text{for } j = l - \frac{1}{2} \right), \tag{28}$$

that  $Y_l^{m\pm 1/2}(\theta, \varphi)$  represents ordinary spherical harmonics. Then the Dirac Eq. (25) can be written in the simplified matrix form

$$\begin{pmatrix} 0 & -\omega \\ \omega & 0 \end{pmatrix} \begin{pmatrix} F^{\pm} \\ G^{\pm} \end{pmatrix} - \frac{\partial}{\partial r_*} \begin{pmatrix} F^{\pm} \\ G^{\pm} \end{pmatrix} + \sqrt{f} \begin{pmatrix} \frac{\kappa_{\pm}}{br} & m \\ m & \frac{\kappa_{\pm}}{br} \end{pmatrix} \begin{pmatrix} F^{\pm} \\ G^{\pm} \end{pmatrix} = 0, \tag{29}$$

with the constant

$$\kappa_{\pm} = \begin{cases} j + \frac{1}{2}, & j = l + \frac{1}{2} \\ -\left( j + \frac{1}{2} \right), & j = l - \frac{1}{2} \end{cases}, \tag{30}$$

which are negative and positive integers.

In order to simplify the radial equations, we consider separately the (+) and (-) cases. For (+), we make a change of variables Chandrasekhar (1983):

$$\begin{pmatrix} \hat{F}^+ \\ \hat{G}^+ \end{pmatrix} = \begin{pmatrix} \sin\left(\frac{\theta_+}{2}\right) & \cos\left(\frac{\theta_+}{2}\right) \\ \cos\left(\frac{\theta_+}{2}\right) & -\sin\left(\frac{\theta_+}{2}\right) \end{pmatrix} \begin{pmatrix} F^+ \\ G^+ \end{pmatrix}, \tag{31}$$

where

$$\theta_+ = \arctan\left(\frac{bmr}{|\kappa_+|}\right). \tag{32}$$

Then Eq. (29) can be written as

$$\begin{aligned} \frac{d}{dr_*} \begin{pmatrix} \hat{F}^+ \\ \hat{G}^+ \end{pmatrix} - \sqrt{f} \sqrt{\left(\frac{\kappa_+}{br}\right)^2 + m^2} \begin{pmatrix} 1 & 0 \\ 0 & -1 \end{pmatrix} \begin{pmatrix} \hat{F}^+ \\ \hat{G}^+ \end{pmatrix} \\ = -\omega \left(1 + \frac{1}{2\omega} f \frac{mb|\kappa_+|}{\kappa_+^2 + b^2 m^2 r^2}\right) \begin{pmatrix} 0 & -1 \\ 1 & 0 \end{pmatrix} \begin{pmatrix} \hat{F}^+ \\ \hat{G}^+ \end{pmatrix}. \end{aligned} \tag{33}$$

We make another coordinate transformation to simplify these equations as

$$\hat{r}_* = r_* + \frac{1}{2\omega} \arctan\left(\frac{bmr}{|\kappa_+|}\right), \tag{34}$$

and then Eq. (33) is changed to be

$$\frac{d}{d\hat{r}_*} \begin{pmatrix} \hat{F}^+ \\ \hat{G}^+ \end{pmatrix} + W_+ \begin{pmatrix} -\hat{F}^+ \\ \hat{G}^+ \end{pmatrix} = \omega \begin{pmatrix} \hat{G}^+ \\ -\hat{F}^+ \end{pmatrix}, \tag{35}$$

where

$$W_+ = \frac{\sqrt{f} \sqrt{\left(\frac{\kappa_+}{br}\right)^2 + m^2}}{1 + \frac{1}{2\omega} f \left(\frac{bm|\kappa_+|}{\kappa_+^2 + b^2 m^2 r^2}\right)}. \tag{36}$$

These equations can be decoupled to

$$\left(-\frac{d^2}{d\hat{r}_*^2} + V_{+1}\right) \hat{F}^+ = \omega^2 \hat{F}^+, \tag{37}$$

$$\left(-\frac{d^2}{d\hat{r}_*^2} + V_{+2}\right) \hat{G}^+ = \omega^2 \hat{G}^+, \tag{38}$$

with

$$V_{+1,2} = \pm \frac{dW_+}{d\hat{r}_*} + W_+^2. \tag{39}$$

Similar to the case of (+), equations for the case (−) can be written as

$$\left(-\frac{d^2}{d\hat{r}_*^2} + V_{-1}\right) \hat{F}^- = \omega^2 \hat{F}^-, \tag{40}$$

$$\left(-\frac{d^2}{d\hat{r}_*^2} + V_{-2}\right) \hat{G}^- = \omega^2 \hat{G}^-, \tag{41}$$

where

$$V_{-1,2} = \pm \frac{dW_-}{d\hat{r}_*} + W_-^2, \tag{42}$$

with

$$W_- = \frac{\sqrt{f} \sqrt{\left(\frac{\kappa_-}{br}\right)^2 + m^2}}{1 - \frac{1}{2\omega} f \left(\frac{bm|\kappa_-|}{\kappa_-^2 + b^2 m^2 r^2}\right)}. \tag{43}$$

We can put the (+) and (−) cases together and simply name the radial equations  $F$  and  $G$ . Correspondingly, the two decoupled equations can be expressed in the form

$$\left(-\frac{d^2}{d\hat{r}_*^2} + V_1\right) \hat{F} = \omega^2 \hat{F}, \tag{44}$$

$$\left(-\frac{d^2}{d\hat{r}_*^2} + V_2\right) \hat{G} = \omega^2 \hat{G}, \tag{45}$$

where

$$V_{1,2} = \pm \frac{dW}{d\hat{r}_*} + W^2, \tag{46}$$

with

$$W = \frac{\sqrt{f} \sqrt{\left(\frac{\kappa}{br}\right)^2 + m^2}}{1 + \frac{1}{2\omega} f \left(\frac{bm|\kappa|}{\kappa^2 + b^2 m^2 r^2}\right)}. \tag{47}$$

Here  $\kappa$  is all positive and negative integers. Positive integers represent the (+) case with

$$\kappa = j + \frac{1}{2} \quad \text{and} \quad j = l + \frac{1}{2}, \tag{48}$$

while negative integers represent the (−) case with

$$\kappa = -\left(j + \frac{1}{2}\right) \quad \text{and} \quad j = l - \frac{1}{2}. \tag{49}$$

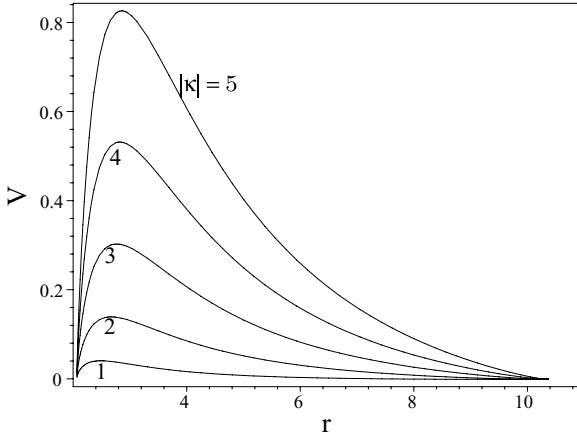


Fig. 7. Variation of the effective potential for Dirac field with  $\Lambda = 0.0225, b = 0.95, m = 0, \kappa = 1, 2, 3, 4, 5$ .

From the Schrödinger-like equations in Eqs. (44) and (45), we can evaluate the QNMs. The forms of  $V_1$  and  $V_2$  shown in Eq. (46) are super-symmetric partners derived from the same super-potential  $W$  Cooper *et al.* (1995). Reference Anderson and Price (1991) has proved that potentials related in this ways have the same spectral of QNMs. So we deal with Eq. (44) with potential  $V_1$  in evaluating the QNMs. The effective potential also depends on  $\omega$ . This will complicate matters in Eq. (12) because there are  $\omega$  dependence on both sides of the equation.

First we analyse the dependence of the effective potential on the parameters  $m, \kappa, b, \Lambda, \omega$ . We can see from the Fig. 7 that the dependence of effective potential on  $\kappa$  of Dirac field is similar to the case of scalar field. In Figs. 9 and 10, we show dependence of the effective potential on other parameters respectively. Compared with the effective potential mentioned in Cho (2002), the most difference is the asymptotic value,

$$\begin{aligned}
 V(r \rightarrow \infty) &= m^2, \text{ Schwarzschild black hole,} \\
 V(r \rightarrow r_c) &= 0, \text{ Schwarzschild de-Sitter black hole.}
 \end{aligned}
 \tag{50}$$

The effective potential remains potential barrier. Tunnelling to occur  $\omega^2$  of the Dirac field must be smaller than the peak value of the potential and the energy of the Dirac field is always larger than the mass  $m$ , so the QNMs exist only when  $m^2 < \omega^2 < V_{\max}$ . We can estimate the maximum value  $m_{\max}$  from Cho (2002):

$$V(r_{\max}, m_{\max}, \kappa, b, \Lambda, \omega = m_{\max}) = (m_{\max})^2.
 \tag{51}$$

We solve it numerically and list the result in Table II, where we give the maximum value of  $\mu = m/\kappa$ . The results suggest that  $\Lambda$  reduce the value of  $\mu_{\max}$ .

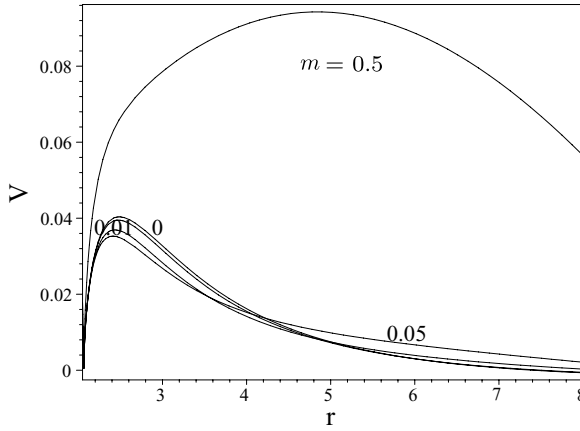


**Fig. 8.** Variation of the effective potential for Dirac field with  $\Lambda = 0.0225, b = 0.95, \omega = 0.1, \kappa = 1, m = 0, 0.01, 0.05, 0.1, 0.5$ .

By writing the potential in Eqs. (46) and (47) as  $V(r, \kappa, m = \kappa\mu, \omega, \Lambda, b)$ , the maximums of  $\mu$  listed in Table II indicate that  $\mu$  can be treated as a small parameter for expansion. We obtain the QNMs in WKB approximation as power series of  $\mu$  for given values of  $\kappa$  Seidel and Iyer (1990); Simone and Will (1992); Cho (2002).

We first express the position of the peak of the effective potential as serial up to order  $\mu^6$ ,

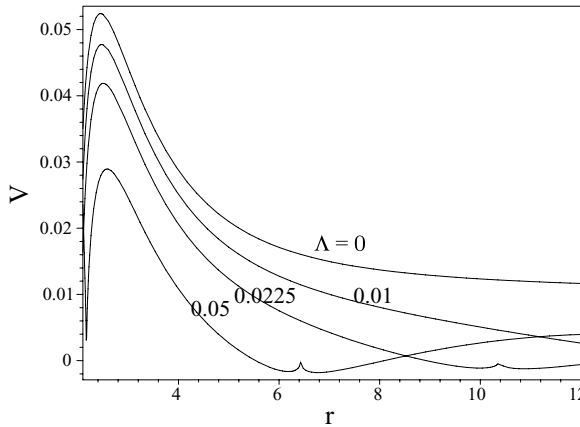


**Fig. 9.** Variation of the effective potential for Dirac field with  $b = 0.95, \omega = 0.1, \kappa = 1, m = 0.1, \Lambda = 0, 0.01, 0.0225, 0.05$ .

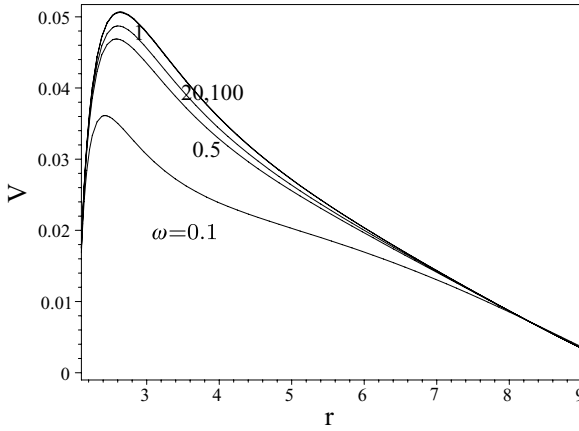


**Fig. 10.** Variation of the effective potential for Dirac field with  $b = 0.95, \Lambda = 0.0225, \kappa = 1, m = 0.1, \omega = 0.1, 0.5, 1, 20, 100$ .

$$\begin{aligned}
 r_{\max} &= r_0 + r_1\mu + r_2\mu^2 + r_3\mu^3 + r_4\mu^4 + r_5\mu^5 + r_6\mu^6 \\
 &= r_0 + \Sigma,
 \end{aligned}
 \tag{52}$$

and

$$\begin{aligned}
 0 &= V'(r_{\max}) \\
 &= V'(r_0) + \Sigma V''(r_0) + \frac{1}{2}\Sigma^2 V'''(r_0) + \frac{1}{6}\Sigma^3 V^{(4)}(r_0) \\
 &\quad + \frac{1}{24}\Sigma^4 V^{(5)}(r_0) + \frac{1}{120}\Sigma^5 V^{(6)}(r_0) + \frac{1}{720}\Sigma^6 V^{(7)}(r_0).
 \end{aligned}
 \tag{53}$$

**Table II.** Maximums of the Mass  $\mu$  of Dirac Field Above Which QNMs Cannot Occur with  $|\kappa| = 1$  to 5 for  $b = 1$

$\kappa$	$\mu_{\max}(\Lambda = 0)$	$\mu_{\max}(\Lambda = 0.0009)$	$\mu_{\max}(\Lambda = 0.0225)$	$\mu_{\max}(\Lambda = 0.09)$
-5	-0.263	-0.260	-0.212	-0.0877
-4	-0.267	-0.264	-0.214	-0.0881
-3	-0.273	-0.270	-0.218	-0.0886
-2	-0.283	-0.283	-0.226	-0.0908
-1	-0.333	-0.330	-0.261	-0.0993
1	0.224	0.223	0.197	0.0932
2	0.226	0.225	0.194	0.0879
3	0.232	0.230	0.196	0.0870
4	0.236	0.234	0.198	0.0867
5	0.238	0.237	0.190	0.0866

**Table III.** Real Parts of the Coefficients of the Expansions in Power of  $\mu$  for the QNMs with  $|\kappa| = 1$  to 5 for  $\Lambda = 0.0225, b = 0.95$

$ \kappa $	$n$	$\text{Re}(\omega_0)$	$\text{Re}(\omega_1)$	$\text{Re}(\omega_2)$	$\text{Re}(\omega_3)$	$\text{Re}(\omega_4)$	$\text{Re}(\omega_5)$	$\text{Re}(\omega_6)$
1	0	0.1693	-0.1453	0.5500	-0.3968	1.283	-5.686	7.796
2	0	0.3575	-0.1300	1.365	0.2497	0.9690	1.915	-0.8212
	1	0.3395	-0.1290	0.7535	-0.7397	0.8720	-12.20	28.53
3	0	0.5402	-0.1275	2.137	0.3908	0.9862	1.538	0.9568
	1	0.5281	-0.1297	1.694	-0.2227	2.726	-1.1013	27.16
	2	0.5069	-0.1260	0.9469	-0.8146	0.2356	-15.35	31.12
4	0	0.7218	-0.1269	2.889	0.4305	0.9627	1.224	-0.07142
	1	0.7128	-0.1286	2.549	0.05743	3.087	1.506	21.15
	2	0.6961	-0.1287	1.932	-0.4737	3.617	-5.224	57.11
	3	0.6735	-0.1248	1.133	-0.8544	-0.5692	-17.01	30.99
5	0	0.9032	-0.1266	3.634	0.4486	0.9623	1.049	-1.252
	1	0.8959	-0.1279	3.359	0.2022	3.034	1.871	15.55
	2	0.8822	-0.1288	2.843	-0.2031	4.873	-0.6548	52.75
	3	0.8631	-0.1277	2.141	-0.6085	3.801	-8.450	77.67
	4	0.8397	-0.1243	1.315	-0.8781	-1.464	-18.00	30.09

Where  $r_0$  is the position of the peak for the massless Dirac field effective potential. From Eq. (47) for the massless Dirac field case, the expression of effective potential  $V$  doesn't depend on  $\omega$  and can be solved independently. We evaluate the coefficients  $r_i$ 's order by solving this equation. The expression of  $r_{\max}$  contains  $\mu$  and unknown  $\omega$  by given  $\Lambda$  and  $b$ . We also expand  $\omega$  as  $\omega = \omega_0 + \omega_1\mu + \omega_2\mu^2 + \omega_3\mu^3 + \omega_4\mu^4 + \omega_5\mu^5 + \omega_6\mu^6$  and plug in the expansion for  $r_{\max}$ , and then expand the derivation of the potential  $V_0^{(n)}$  performed with respect to  $\hat{r}_*$ . We plug all these expansions back to Eq. (12) and can solve the coefficients  $\omega_i$ 's self-consistently order by order in  $\mu$ . We list the results of  $\Lambda = 0.0225, b = 0.95$  by taking four significant digits in Tables III and IV.

We check the QNMs for  $\kappa = 1$  and  $n = 0$ . For  $m = 0$ ,

$$\omega = \omega_0 = 0.1693 - 0.08800i, \tag{54}$$

for  $m = 0.1$ ,

$$\begin{aligned} \omega_0 &= 0.1693 - 0.08800i, \\ \omega_1 m &= -0.01453 - 0.003811i, \\ \omega_2 m^2 &= 0.005500 + 0.003871i, \\ \omega_3 m^3 &= -0.0003968 + 0.0006175i, \\ \omega_4 m^4 &= 0.0001283 + 0.00004488i, \\ \omega_5 m^5 &= -0.00005686 - 0.00008623i, \\ \omega_6 m^6 &= 0.000007796 - 0.00003765i, \end{aligned} \tag{55}$$



**Table IV.** Imaginary Parts of the Coefficients of the Expansions in Power of  $\mu$  for the QNMs with  $|\kappa| = 1$  to 5 for  $\Lambda = 0.0225$ ,  $b = 0.95$

$ \kappa $	$n$	$\text{Im}(\omega_0)$	$\text{Im}(\omega_1)$	$\text{Im}(\omega_2)$	$\text{Im}(\omega_3)$	$\text{Im}(\omega_4)$	$\text{Im}(\omega_5)$	$\text{Im}(\omega_6)$
1	0	-0.08800	-0.03811	0.3871	0.6175	0.4488	8.6228	-37.65
2	0	-0.08601	-0.01095	0.4560	0.4640	0.03789	2.051	-2.386
	1	-0.2633	-0.04504	1.139	0.2860	4.248	6.265	65.59
3	0	-0.08594	-0.006818	0.4609	0.3150	-0.3549	0.5060	-4.262
	1	-0.2600	-0.02478	1.280	0.5967	2.126	6.472	15.88
	2	-0.4383	-0.04651	1.858	0.1927	8.767	5.456	170.6
4	0	-0.08593	-0.005024	0.4623	0.2377	-0.5267	0.1351	-4.982
	1	-0.2590	-0.01697	1.330	0.5659	0.6092	3.533	-1.387
	2	-0.4348	-0.03195	2.046	0.5232	5.892	8.076	73.49
	3	-0.6134	-0.04752	2.575	0.1428	13.40	4.760	261.0
5	0	-0.08593	-0.003991	0.4629	0.1907	-0.6117	0.01554	-5.211
	1	0-0.2585	-0.01296	1.352	0.4946	-0.2976	1.922	-8.361
	2	-0.4330	-0.02393	2.140	0.5962	3.4529	6.184	28.29
	3	-0.6098	-0.03619	2.788	0.4427	10.18	8.220	145.6
	4	-0.7886	-0.04830	3.290	0.1094	18.00	4.199	346.0

taking three significant digits, both the real and imaginary parts of  $\omega\mu^4$  and higher order do not contribute to the frequency, so

$$\omega = 0.160 - 0.0872i \tag{56}$$

is accurate up to at least three significant digits.

For  $m = 0.2$ ,

$$\begin{aligned} \omega_0 &= 0.1693 - 0.08800i, \\ \omega_1 m &= -0.02905 - 0.007621i, \\ \omega_2 m^2 &= 0.02200 + 0.01548i, \\ \omega_3 m^3 &= -0.003175 + 0.004940i, \\ \omega_4 m^4 &= 0.002053 + 0.0007181i, \\ \omega_5 m^5 &= -0.001820 - 0.002759i, \\ \omega_6 m^6 &= 0.0004989 - 0.002410i, \end{aligned} \tag{57}$$

and

$$\omega = 0.160 - 0.0741i. \tag{58}$$

We see that the highest order  $\omega m^6$  will contribute to  $\omega$ . Requiring result to be three significant digits, we need to consider the higher orders than  $\mu^6$ . But we expand terms up to  $\mu^6$ , so we disregard this result for  $m = 0.2$ , though there should be a QNMs around this value.

For different values of  $\kappa$  and  $n$ , we calculate QNMs of  $m = 0, 0.1, 0.2, 0.5$  and plot the results in Fig. 11 expect the results which three significant digits

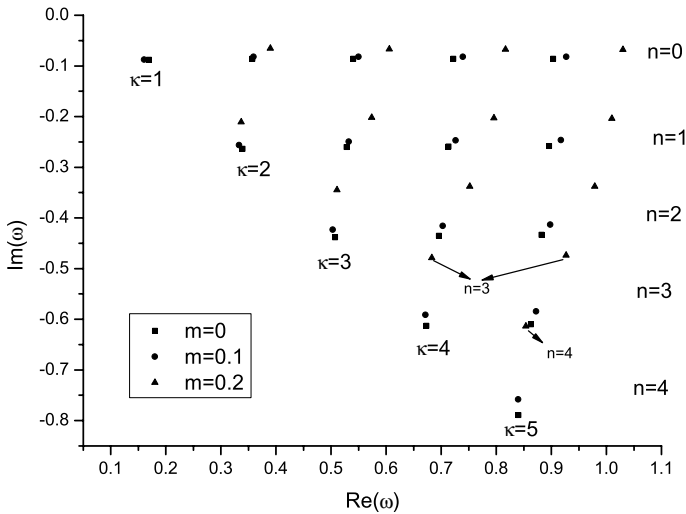


Fig. 11. QNMs of Dirac field for  $\Lambda = 0.0225, b = 0.95$ .

accuracy cannot be maintained with terms expanded up to  $\mu^6$ . Increasing of mass of Dirac fields leads to the real parts of QNMs increase and imaginary parts decrease. In Table V and Fig. 12, we list and plot the QNMs for different  $\Lambda$  and  $b$ ,  $\Lambda$  makes both real and magnitude of imaginary parts of QNMs decrease;  $b$  makes the real parts increase and makes the magnitude of imaginary parts decrease.

Table V. QNMs of Dirac Field for  $m = 0.1, b = 1$

$ \kappa $	$n$	$\Lambda = 0$	$\Lambda = 0.0009$	$\Lambda = 0.0225$	$\Lambda = 0.09$
1	0	0.164-0.102i	0.164-0.102i	0.149-0.0879i	
2	0	0.377-0.0922i	0.375-0.0917i	0.339-0.0816i	0.172-0.0408i
	1	0.344-0.296i	0.342-0.293i	0.312-0.256i	0.138-0.123i
3	0	0.581-0.0908i	0.579-0.0904i	0.522-0.0812i	0.259-0.0410i
	1	0.556-0.282i	0.555-0.281i	0.503-0.248i	0.258-0.123i
	2	0.518-0.489i	0.516-0.487i	0.473-0.423i	0.255-0.206i
4	0	0.783-0.0903i	0.781-0.0898i	0.703-0.0812i	0.347-0.0411i
	1	0.764-0.275i	0.761-0.275i	0.688-0.245i	0.346-0.123i
	2	0.730-0.473i	0.727-0.471i	0.664-0.415i	0.344-0.206i
	3	0.691-0.683i	0.688-0.680i	0.631-0.589i	0.341-0.288i
5	0	0.985-0.0900i	0.982-0.0897i	0.884-0.0811i	0.435-0.0412i
	1	0.970-0.272i	0.966-0.272i	0.871-0.244i	0.434-0.123i
	2	0.941-0.465i	0.937-0.464i	0.852-0.411i	0.433-0.206i
	3	0.903-0.667i	0.899-0.664i	0.823-0.584i	0.429-0.289i
	4	0.864-0.877i	0.861-0.871i	0.790-0.756i	0.426-0.371i

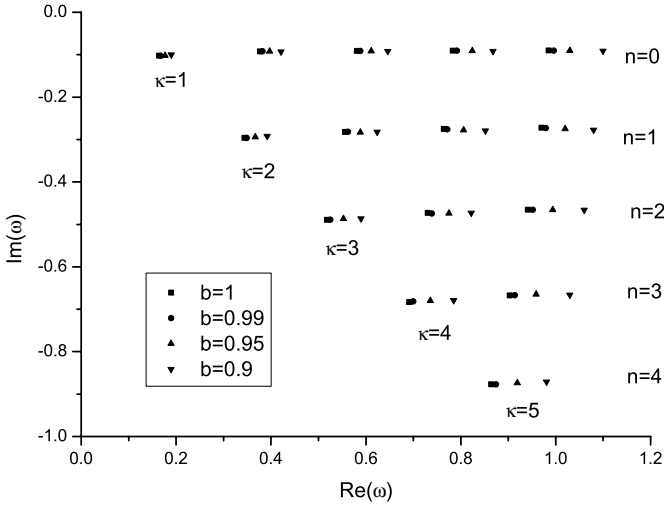


Fig. 12. QNMs of Dirac field for  $m = 0.1, \Lambda = 0$ .

4. DISSCUSSION AND CONCLUSION

We have evaluated both scalar and Dirac low-lying QNMs of a Schwarzschild-de Sitter black hole with a global monopole, using the WKB approximation. For the massive Dirac field, we adopt a further approximation by making perturbative expansions for all the quantities in powers of parameter  $\mu$ . In this way, we can obtain QNMs up to three significant digits.

In general, the real parts of QNMs increase with  $l$  for scalar field and with  $\kappa$  for Dirac field, but they decrease with mode number  $n$  for fixed  $l$  or  $\kappa$ . The magnitudes of the imaginary parts increase with  $n$ . The mass of the field makes the real parts of QNMs increase and makes the imaginary parts decrease Simone and Will (1992); Cho (2002). From Figs. 5 and 11, we find the influence of mass on QNMs is different for scalar and Dirac fields. For larger quantum number  $l$ , the influence of mass to the real parts of scalar QNMs is smaller, but the other way round for Dirac case. The cosmological constant  $\Lambda$  reduces the magnitudes of maximum mass of Dirac field for fixed  $\kappa$ , and decreases both the real and magnitude of imaginary parts of QNMs of scalar and Dirac fields. From the Eqs. (9) and (47), we see that  $b$  is a factor of  $\kappa$  or  $l$  which can increase the magnitudes little, so  $b$  increases the real parts of the QNMs and decreases the magnitudes of the imaginary parts.

All the QNMs above are measured in units of the black hole mass  $M$ . To convert those to  $Hz$  must multiply by  $32310 \frac{M_{\odot}}{M}$ . For a one solar mass black hole,  $\omega = 0.160 - 0.0872i$  is corresponding to ringing frequency  $32310 \times 0.160 = 5.17 kHz$  and a damping timescale  $\tau = \frac{1}{32310 \times 0.0872} = 3.55 \times 10^{-4} s$ .

We can use WKB methods to other black holes. All these efforts will enrich our knowledge about QNMs of different kind of black holes and give direct identification to distinguish the kind of black holes, through gravitational wave detectors in the future.

## ACKNOWLEDGMENTS

The work has been supported by the National Natural Science Foundation of China (Grant No. 10273017), (Grant No. 10573027) and Science Foundation of Shanghai (Grant No. 05ZR14138). J. F. Chang thanks Dr. Xiang Li and Xian-Hui Ge for their zealous help during the work.

## REFERENCES

- Anderson, A. and Price, R. H. (1991). *Physical Review D* **43**, 3147.
- Barriola, M. and Vileikin, A. (1989). *Physical Review Letters* **63**, 341.
- Bjorken, J. D. and Drell, S. D. (1964). *Relativistic Quantum Mechanics*, McGraw Hill.
- Brady, P., Chambers, C., Krivan, W., and Laguna, P. (1997). *Physical Review D* **55**, 7538.
- Brady, P., Chambers, C., Laarakkers, W., and Poisson, E. (1999). *Physical Review D* **60**, 064003.
- Brill, D. R. and Wheeler, J. A. (1957). *Rev. Mod. Phys.* **29**, 465.
- Cardoso, V. and Lemos, J. P. (2001). *Physical Review D* **64**, 084017.
- Cardoso, V. and Lemos, J. P. S. (2003). *Physical Review D* **67**, 084020.
- Chandrasekhar, S. (1983). *The Relativistic Quantum Mechanics*, Clarendon Press.
- Chang, J. F. and Shen, Y. G. (2005). *Nucl. Phys. B* **712**, 347.
- Cho, H. T. (2003). *Physical Review D* **68**, 024003.
- Cooper, F., Khare, A., and Sukhatme, U. (1995). *Phys. Rept.* **251**, 267.
- Dadhich, N., Narayan, K., and Yajnik, U. A. (1998). *Pramana-Journal of Physics* **50**, 307.
- Horowitz, D. T. and Gubeny, V. (1999). *Physical Review D* **62**, 024027.
- Iyer, S. and Will, C. M. (1987). *Physical Review D* **35**, 3621.
- Iyer, S. (1987). *Physical Review D* **35**, 3632.
- Iyer, S. (1990). *Physical Review D* **41**, 374.
- Jing, J. L. (2004). *Physical Review D* **69**, 084009.
- Kokkotas, K. and Schmidt, B. (1999). *Living Reviews Relative* **2**, 2.
- Maassen, A van den Brink (2003). *Physical Review D* **68**, 047501.
- Mellor, F. and Moss, I. G. (1990). *Physical Review D* **41**, 403.
- Molina, C. (2003). *Physical Review D* **68**, 064007.
- Moss, I. G. and Norman, J. P. (2002). *Class. Quant. Grav.* **19**, 2323.
- Moss, I. G. and Norman, J. P. (2002). *Class. Quantum. Grav.* **19**, 2323.
- Nollert, H. P. (1999). *Class. Quant. Grav.* **16**, R159.
- Schutz, B. F. and Will, C. M. (1985). *Astrophys. J. Lett.* **291**, L33.
- Seidel, E. and Iyer, S. (1990). *Physical Review D* **41**, 374.
- Shen, Y. G. and Chen, D. M. (1998). *Nuovo Cimento.* **B113**, 1273.
- Simone, L. E. and Will, C. M. (1992). *Class. Quantum. Grav.* **9**, 963.
- Suneeta, V. (2003). *Physical Review D* **68**, 024020.
- Yu, H. W. (2002). *Physical Review D* **65**, 087502.
- Zhidenko, A. (2004). *Class. Quant. Grav.* **21**, 273.